



Novel non-peptidic vinylsulfones targeting the S2 and S3 subsites of parasite cysteine proteases

Clifford Bryant^{a,b}, Iain D. Kerr^d, Moumita Debnath^d, Kenny K. H. Ang^{a,b}, Joseline Ratnam^{a,b}, Rafaela S. Ferreira^c, Priyadarshini Jaishankar^{a,b}, DongMei Zhao^{a,b}, Michelle R. Arkin^{a,b,c}, James H. McKerrow^{b,e}, Linda S. Brinen^{b,d}, Adam R. Renslo^{a,b,c,*}

^a Small Molecule Discovery Center, University of California, San Francisco, CA 94158, United States

^b Sandler Center for Basic Research on Parasitic Disease, University of California, San Francisco, CA 94158, United States

^c Department of Pharmaceutical Chemistry, University of California, San Francisco, CA 94158, United States

^d Department of Cellular and Molecular Pharmacology, University of California, San Francisco, CA 94158, United States

^e Department of Pathology, University of California, San Francisco, CA 94158, United States

ARTICLE INFO

Article history:

Received 12 July 2009

Accepted 31 August 2009

Available online 3 September 2009

Keywords:

Protease inhibitors

Cruzain

Rhodesain

Vinylsulfone

ABSTRACT

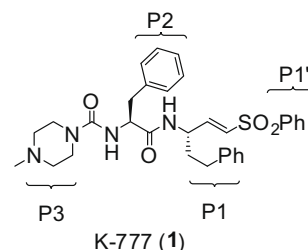
We describe here the identification of non-peptidic vinylsulfones that inhibit parasite cysteine proteases in vitro and inhibit the growth of *Trypanosoma brucei* parasites in culture. A high resolution (1.75 Å) co-crystal structure of **8a** bound to cruzain reveals how the non-peptidic P2/P3 moiety in such analogs bind the S2 and S3 subsites of the protease, effectively recapitulating important binding interactions present in more traditional peptide-based protease inhibitors and natural substrates.

© 2009 Elsevier Ltd. All rights reserved.

There is an urgent need for new safe and effective drugs to treat the trypanosomal diseases such as Human African Trypanosomiasis (HAT) and Chagas' disease. Existing drugs for these conditions are sub-optimal with regard to efficacy and/or safety, while the lone truly modern drug available for HAT, eflornithine, is difficult to administer in poor rural settings, and is effective only against *Trypanosoma brucei gambiense*. Current efforts to address this unmet medical need range from the repurposing of azole antifungals¹ in Chagas' disease to the investigation of a variety of recently identified biochemical targets.^{2,3} Prominent among the latter are papain-like cysteine proteases such as cruzain in *Trypanosoma cruzi* and rhodesain and TbCatB in *Trypanosoma brucei*.⁴ There is now good precedent for targeting cysteine proteases in human disease seeing as inhibitors of related human proteases have progressed into late stage clinical trials (e.g., cathepsin K inhibitor odanacatib⁵ for osteoporosis). Among parasite protease inhibitors being studied is the cruzain inhibitor K777 (**1**), currently in preclinical development as a potential treatment for Chagas' disease.⁶

Classical cysteine protease inhibitors comprise a di- or tripeptide linked to an electrophilic warhead that engages the active-site cysteine thiol function reversibly or irreversibly. Such inhibitors readily recapitulate the binding interactions of endogenous substrate (pri-

marily hydrophobic and hydrogen bonding interactions), but as peptides also possess well recognized liabilities as potential drugs. These include susceptibility to enzymatic or chemical hydrolysis of peptide bonds and the metabolism of amino acid side chains, issues that can potentially be addressed through chemical modification of the amino acid backbone and/or side chain. We describe here our initial efforts to identify non-peptidic parasite cysteine protease inhibitors that recapitulate the binding interactions of substrate-like peptidic inhibitors but have a greater likelihood of possessing drug-like properties.



Recently, Ellman and co-workers described a non-peptidic class of cruzain inhibitors discovered via the 'substrate activity screening' approach advanced by that lab.⁷ In the work described here, we similarly aimed to survey non-peptidic fragments as potential P2/P3 moieties, but proceeded by screening the inhibitors directly.

* Corresponding author.

E-mail address: adam.renslo@ucsf.edu (A.R. Renslo).

While empirical in nature, this effort was guided by the availability of co-crystal structures of substrate-like inhibitors bound to cruzain.^{8,9} Inspection of these structures suggested to us that an aliphatic or heterocyclic ring might serve as a non-peptidic linkage to a second pendant hydrophobe that would bind in the enzyme's S2 pocket, playing a role analogous to the phenylalanine side chain in inhibitors like **1**. To explore this possibility, carboxylic acids meeting the above design criteria were acquired from commercial sources and coupled to the known vinylsulfone amine **2**,¹⁰ as illustrated below for a representative series of (hetero)aryl thiazoles (**3a–c**, Scheme 1).

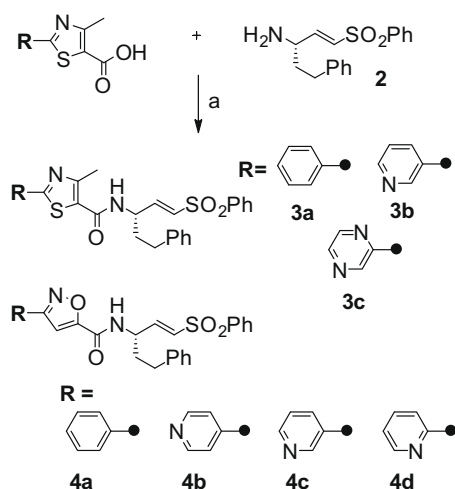
Around 30 non-peptidic vinylsulfones were prepared and IC₅₀ values determined for cruzain, rhodesain, and TbCatB (5 min incubation with inhibitor). True rate constants of rhodesain inactivation were subsequently determined for the most potent analogs (Table 1).^{11,12} A broad range of potencies were observed for these analogs and some general SAR trends could be discerned. Analogs bearing a single heteroaromatic ring system were generally devoid of enzyme activity (<5% inhibition of cruzain at 1 μM, data not

shown). Similarly ineffective were analogs with a heterocyclic ring linked to a hydrophobe at the ortho position (**5** and **6**, Fig. 1). In contrast, analogs possessing more prolate geometries (e.g., **3a–c**) were found to be effective inhibitors of cruzain and quite potent inhibitors of rhodesain. For example, analog **3a** inhibited rhodesain with IC₅₀ and K_i values superior to those of **1** (Table 1).

We next synthesized a series of similar analogs (**4a–d**) in which an isoxazole ring replaces the thiazole ring of **3a–d** (Scheme 1). For these analogs, the requisite isoxazole carboxylic acid starting materials were prepared in three steps, employing the [3+2] dipolar cycloaddition of nitrile oxides (generated in situ from the hydroximinoyl chlorides¹³) with methyl propiolate as a key step (Scheme 1). The isoxazole analogs **4a–d** exhibited a similar SAR profile as seen for **3a–c**, inhibiting rhodesain more potently than cruzain and conferring no significant inhibition of TbCatB.

The analogs **7a/b** and **8a/b** represent a second and structurally distinct series of protease inhibitors that emerged from our survey of non-peptidic P2/P3 fragments (Fig. 2). These analogs were prepared as diastereomeric mixtures from the coupling of (±) *trans*-2-(4-chlorobenzoyl)cyclohexane-1-carboxylic acid to vinylsulfone amines. We successfully separated the two diastereomers of **7** and found that one isomer was at least 100-fold more potent than the other, an encouraging result that implied specific binding interactions, presumably involving the S2 and/or S3 subsites of the protease active-site.

To better understand the binding mode of analogs such as **7** and **8**, we crystallized cruzain inhibited by **7** or **8** (as diastereomeric mixtures). Cruzain inhibited by **8** provided superior crystals and so we collected diffraction data for these at the Stanford Synchrotron Radiation Lightsource (SSRL), BL7-1 (Table 2). Traditionally, recombinant cruzain has been expressed in *Escherichia coli* and purified from refolded inclusion bodies. However, in our experience the final yield of protein was typically in the low milligram



Scheme 1. Synthesis of non-peptidic vinylsulfones **3a–c** from commercially available acids. Reagents and conditions: (a) **2**-HCl, HATU, DIEA, DMF, rt. The preparation of isoxazoles **4a–d** was accomplished from commercially available isoxazole acids (for **4a**) or from pyridyl aldehydes as follows for the case of **4d**. Reagents and conditions: (a) 2-pyridinecarboxaldehyde, NH₂OH, NaOAc, 95% EtOH, reflux, 71%; (b) NCS, DMF, 50 °C, then methyl propiolate, Et₃N, CH₂Cl₂, rt, 69%; (c) 1.0 M LiOH, MeOH–THF; (d) **2**-HCl, HATU, DIEA, DMF, rt; 81% over two steps.

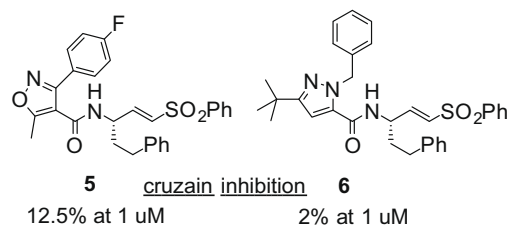


Figure 1. Representative examples of ineffective vinylsulfone analogs from the initial survey of non-peptidic P2/P3 moieties.

Table 1
Enzymatic and biological activities of vinylsulfone analogs

Compd	Protease inhibition IC ₅₀ (μM)			Rhodesain inhibition kinetics ¹²			Parasite growth inhibition GI ₅₀ (μM)	Cytotoxicity IC ₅₀ (μM)
	Cruzain	Rhodesain	TbCatB	k _{inact} /K _i (M ^{−1} s ^{−1})	K _{i,app} (μM)	k _{inact} (s ^{−1})	<i>T. b. b</i> parasites	Jurkat cells
K-777 (1)	0.004	0.007	4	555,000	0.78	0.029	7	3% at 10 μM
3a	10	<0.006	>100	84,000	0.32	0.0018	>100	>100
3b	2	0.03	>100	20,100 ^a	—	—	20	98
3c	1	0.01	>100	25,200	4.77	0.0079	7	>100
4a	2	0.01	40	3610	13.0	0.0031	>100	>100
4b	5	0.05	>100	8590	16.2	0.0091	10	>100
4c	1	0.01	>100	348,000 ^a	—	—	>100	>100
4d	6	0.05	>100	7720	7.4	0.0038	10	>100
7a	0.05	0.1	16	9750	0.80	0.00051	12 ^b	>100 ^b
7b	>100	56	>100	2160	4.9	0.0007	nd	nd
8a/b	0.1	0.1	45	5740	38	0.014	8	>100

TbCatB: cathepsin B-like protease in *T. brucei*.

nd = not determined.

^a Value shown is k_{ass}.

^b Tested as the mixture **7a/b**.

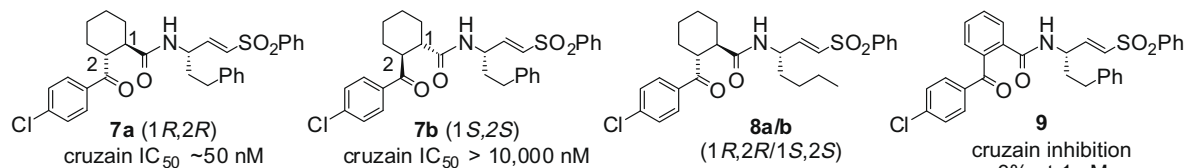


Figure 2. Structures of selected non-peptidic vinylsulfones.

Table 2
X-ray diffraction data and structure refinement statistics

<i>Data collection</i>	
Space group	<i>P</i> 2 ₁
<i>Cell dimensions</i>	
<i>a</i> (Å)	44.69
<i>b</i> (Å)	72.49
<i>c</i> (Å)	60.93
α (°)	90.0
β (°)	89.8
γ (°)	90.0
Resolution (Å)	1.75 (1.84–1.75)
<i>R</i> _{merge} ^a (%)	5.7 (13.7)
<i>I</i> / σI	25 (12)
Completeness (%)	97.3 (90.0)
Redundancy	7.4 (7.2)
Wilson B-factor (Å ²)	11.5
<i>Refinement</i>	
<i>R</i> _{free} / <i>R</i> _{factor} (%)	17.6/14.3
Average B-factor (Å ²)	4.46
<i>Rms deviations</i>	
Bond lengths (Å)	0.019
Bond angles (°)	1.59
<i>Ramachandran plot</i> ^b	
Favored (%)	97.2
Allowed (%)	100
Outliers (%)	0
PDB ID	3HD3

^a $R_{\text{merge}} = \sum \sum |I(hj) - \langle I(h) \rangle| / \sum \sum I(hj)$, where $I(h)$ is the measured diffraction intensity and the summation includes all observations.

^b As defined by Molprobit.¹⁶

range from a multi-liter culture. More recently, we transitioned to an expression system in the yeast *Pichia pastoris* that produces 10–20 mg of soluble cruzain from four liters of culture. The gene encoding cruzain was engineered to accommodate mutations at two predicted glycosylation sites, Ser49Ala and Ser172Gly (mature domain numbering), preventing the need for deglycosylation of the yeast-expressed protein.

The covalently inhibited complex crystallized with two molecules of the mature domain in the asymmetric unit that superimpose 214 matching α -carbons with root mean square distances (rmsd) of 0.34 Å. The high resolution of the diffraction data (1.75 Å) allowed us to assign the absolute configuration of the active diastereomer **8a** (and by extension **7a**) as 1*R*,2*R* at the P2 cyclohexane ring (both diastereomers possess the *S* configuration at P1). Inspection of the cruzain-**8a** structure reveals that the cyclohexane ring in **8a** is located in the S2 subsite of the cruzain active site while the chlorophenyl ring extends over to form hydrophobic contact with the S3 subsite (Fig. 3). The importance of cyclohexane ring stereochemistry in **7/8** is further supported by the finding that the benzophenone congener **9** (Fig. 2) does not significantly inhibit cruzain (3% inhibition at 1 μM). Apparently a flat aromatic P2 substituent as found in **9** is unable to form favorable contacts with the S2 pocket and/or cannot not properly direct the pendant chlorophenyl moiety towards the S3 subsite.

Superimposition of our coordinates for cruzain-**8a** with our earlier cruzain-(**1**) crystal structure (PDB ID 2OZ2) reveals a number of

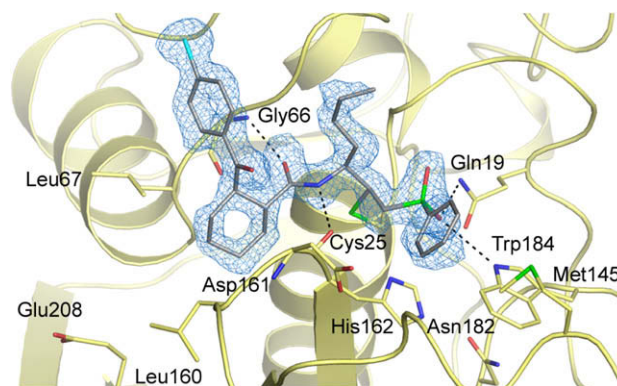


Figure 3. The crystal structure of the cruzain-**8a** complex, solved to a resolution of 1.75 Å. The inhibitor is colored gray and the unbiased mFo-DFc electron density is shown in blue.

conserved interactions in the S1, S1', and S2 subsites. These include the formation of two hydrogen bonds to the inhibitor backbone and another two with the sulfone moiety in the S1' subsite of the enzyme. Conversely, the presence of a non-peptidic group at P2 in **8a** results in the loss of a hydrogen bonding interaction to the inhibitor backbone that is present in the cruzain complex with **1**. With respect to S3, the non-peptidic P3 moieties of **1** (*N*-methyl piperazine) and **8a** (4-chlorophenyl) do not make any direct or water-mediated polar contacts with the enzyme (within a 3.5 Å cut-off). However, a number of non-polar residues contribute to the binding of **1** and **8a** at the S3–S1' subsites, including Gly65 and Gly 66 at S3, Leu67, Ala138, and Leu160 at S2, Gly23 at S1, and Met145 at S1'. As observed in other structures of cruzain bound by inhibitors with non-polar P2 substituents, the 'specificity' residue at the bottom of the S2 subsite (Glu208) points away from the S2 pocket. Only in the presence of basic and polar P2 groups (e.g., Arg) is Glu208 seen to point into the S2 subsite to interact directly with the bound small molecule.⁸

Non-peptidic inhibitors possessing reasonable enzymatic activity were subsequently tested for their ability to inhibit the growth of cultured *T. brucei brucei* parasites and for general cytotoxicity to mammalian cells (Jurkat). Gratifyingly, many of the non-peptidic vinylsulfones were nearly as effective as **1** against cultured parasites, while conferring no significant toxicity to Jurkat cells. With respect to the anti-parasite effects of **3** and **4**, the presence of a nitrogen atom in the pendant aryl ring seems to be important. Hence phenyl substituted analogs **3a** and **4a** were ineffective against cultured parasites while pyridyl (**3b**, **4b**, **4d**) and pyridazyl (**3c**) analogs exhibited antiparasitic effects at low micromolar concentration. Interestingly, in our earlier study of non-basic analogs of **1**, a P3 2-pyridyl analog was found to be more effective against culture *T. cruzi* parasites than non-pyridyl analogs with superior enzyme activity.¹⁴ Since none of these analogs are predicted to be significantly protonated at cytosolic or lysosomal pH, protonation state cannot explain the superior parasite activities of the heteroatom substituted analogs. The effect instead might reflect intrinsic membrane permeability and/or active transport into par-

asite. Adenosine transporters from *Trypanosoma brucei* are implicated in the pharmacology of a number of antitrypanosomals, for example.¹⁵

Vinylsulfone analogs **7** and **8** were also examined in the cell-based assays and found to exhibit anti-parasite effects comparable to **1** against *T. brucei brucei* parasites, without significant cytotoxicity to Jurkat cells (Table 1). These analogs were tested as diastereomeric mixtures, and so one expects that the active diastereomers **7a** and **8a** should be as much as twice as potent against parasites. While siRNA studies have implicated TbCatB as an important target in *T. brucei* parasites, the analogs described herein exert a significant anti-parasitic effect even in the absence of notable in vitro activity against this enzyme. As irreversible inhibitors however, one cannot rule out inhibition of TbCatB by **3**, **4**, **7**, or **8** in the context of parasite culture where the time scale of exposure is much longer than in a biochemical assay.

In summary, two new classes of non-peptidic vinylsulfone-based cysteine protease inhibitors have been discovered using an empirical but structure-guided approach. Many of the non-peptidic analogs exhibit enzyme and parasite activities comparable to more traditional peptidic inhibitors and none of the non-peptidic species were significantly cytotoxic to Jurkat (mammalian) cells. A co-crystal structure of the non-peptidic vinylsulfone **8a** (SMDC-256047) bound to cruzain has been solved to high resolution, demonstrating effective binding to S1'–S3 subsites of cruzain. To our knowledge, this is the first co-crystal structure of a non-peptidic inhibitor bound to cruzain and this structure should greatly facilitate the design of more drug-like parasite cysteine protease inhibitors.

Acknowledgements

This work was generously supported by funding from the Sandler Foundation (to A.R.R. and L.S.B.), and the QB3-Malaysia Program (to K.H.H.A.). We thank Dr. P. Vedantham for re-synthesizing a sample of **7a**. Part of this research was performed at the Stanford Synchrotron Radiation Lightsource (SSRL), a national user facility operated by Stanford University on behalf of the U.S. Department of Energy, Office of Basic Energy Sciences. The SSRL Structural Molecular Biology Program is supported by

the Department of Energy, Office of Biological and Environmental Research, and by the National Institutes of Health, National Center for Research Resources, Biomedical Technology Program, and the National Institute of General Medical Sciences.

References and notes

- Benaim, G.; Sanders, J. M.; Garcia-Marchan, Y.; Colina, C.; Lira, R.; Caldera, A. R.; Payares, G.; Sanoja, C.; Burgos, J. M.; Leon-Rossell, A.; Concepcion, J. L.; Schijman, A. G.; Levin, M.; Oldfield, E.; Urbina, J. A. *J. Med. Chem.* **2006**, 49(3), 892.
- Frearson, J. A.; Wyatt, P. G.; Gilbert, I. H.; Fairlamb, A. H. *Trends Parasitol.* **2007**, 23, 589.
- Renslo, A. R.; McKerrow, J. H. *Nat. Chem. Biol.* **2006**, 2, 701.
- Sajid, M.; McKerrow, J. H. *Mol. Biochem. Parasitol.* **2002**, 120, 1.
- Gauthier, J. Y.; Chauret, N.; Cromlish, W.; Desmarais, S.; Duong, Ie, T.; Falgout, J. P.; Kimmel, D. B.; Lamontagne, S.; Leger, S.; LeRiche, T.; Li, C. S.; Masse, F.; McKay, D. J.; Nicoll-Griffith, D. A.; Oballa, R. M.; Palmer, J. T.; Percival, M. D.; Riendeau, D.; Robichaud, J.; Rodan, G. A.; Rodan, S. B.; Seto, C.; Therien, M.; Truong, V. L.; Venuti, M. C.; Wesolowski, G.; Young, R. N.; Zamboni, R.; Black, W. C. *Bioorg. Med. Chem. Lett.* **2008**, 18, 923.
- Engel, J. C.; Doyle, P. S.; Hsieh, I.; McKerrow, J. H. *J. Exp. Med.* **1998**, 188, 725.
- Brak, K.; Doyle, P. S.; McKerrow, J. H.; Ellman, J. A. *J. Am. Chem. Soc.* **2008**, 130, 6404.
- Gillmor, S. A.; Craik, C. S.; Fletterick, R. J. *Protein Sci.* **1997**, 6, 1603.
- Brinen, L. S.; Hansell, E.; Cheng, J.; Roush, W. R.; McKerrow, J. H.; Fletterick, R. J. *Structure* **2000**, 8, 831.
- Somoza, J. R.; Zhan, H.; Bowman, K. K.; Yu, L.; Mortara, K. D.; Palmer, J. T.; Clark, J. M.; McGrath, M. E. *Biochemistry* **2000**, 39, 12543.
- Tian, W. X.; Tsou, C. L. *Biochemistry* **1982**, 21, 1028.
- Rhodesain (4 nM) in 100 μ l assay buffer was added to inhibitor dilutions in 100 μ l of 10 μ M Z-FR-AMC in the same buffer. Progress curves were determined for 360 s at room temperature for inhibitor concentrations ranging from 100 to 0.003 μ M. Inhibitor dilutions that gave simple exponential progress curves over a wide range of k_{obs} were used to determine kinetic parameters. The value of k_{obs} , the rate constant for loss of enzymatic activity, was determined from an equation for pseudo first order dynamics using Prism 4 (GraphPad). When k_{obs} varied linearly with inhibitor concentration, k_{ass} was determined by linear regression analysis. If the variation was hyperbolic, k_{inact} and K_i were determined from an equation describing two-step irreversible inhibitor mechanism [$k_{obs} = k_{inact}[I]_0 / ([I]_0 + K_i(1 + [S]_0/K_m))$] and non-linear regression analysis.
- Liu, K.-C.; Shelton, B. R.; Howe, R. K. *J. Org. Chem.* **1980**, 45, 3916.
- Jaishankar, P.; Hansell, E.; Zhao, D. M.; Doyle, P. S.; McKerrow, J. H.; Renslo, A. R. *Bioorg. Med. Chem. Lett.* **2008**, 18, 624.
- De Koning, H. P.; Jarvis, S. M. *Mol. Pharmacol.* **1999**, 56, 1162.
- Davis, I. W.; Leaver-Fay, A.; Chen, V. B.; Block, J. N.; Kapral, G. J.; Wang, X.; Murray, L. W.; Arendall, W. B., 3rd; Snoeyink, J.; Richardson, J. S.; Richardson, D. C. *Nucleic Acids Res.* **2007**, 35, W375.